Nano-Electrodeposits on MEMS Directional Microphones for Hearing Aid Optimization

Sang-Soo Je, Jeonghwan Kim, Michael N. Kozicki, and Junseok Chae

Department of Electrical Engineering, Arizona State University, sje01@asu.edu

ABSTRACT

We present an *in-situ* method for MEMS (micro-electromechanical systems) microphone sensitivity optimization via the growth/retraction of nano-electrodeposits to achieve high directionality in hearing aid applications. Using a DC bias at room temperature, nano-electrodeposits are electrochemically deposited and dissolved on a Ag-doped Ge-Se solid electrolyte film on a microphone diaphragm. The growth and retraction of the nano-electrodeposits generate mass/stress redistribution on the diaphragm, tuning the microphone sensitivity to incoming acoustic sources. Acoustic measurements demonstrate that the directional microphone can achieve a 1.3 dB Directivity Index (DI) improvement upon nano-electrodeposit growth and 0.9 dB DI reversal on nano-electrodeposit retraction.

Keywords: micro-electromechanical systems microphone, nano-electrodeposits growth and retraction, sensitivity adjustment, sensitivity tuning, directivity index.

1 INTRODUCTION

The most common complaint of hearing aid wearers is poor response in noisy environments [1]. Hearing aids should therefore be directional to suppress unwanted acoustic sources [2]. Inadequate fitting to the hearing aid wearer results in poor directionality and degrades the overall performance due to sensitivity mismatch in multiple microphones [3]. Moreover, the sensitivity may drift over time, causing a mismatch that is not present at the time the hearing aids is manufactured [4]. Generally, manufacturers match microphones manually under laboratory conditions, which improves directionality, but associated operational and manufacturing costs are substantial. In order to calibrate the relative outputs from the two microphones, advanced DSP circuits can be used which add gain at the output of one of the microphones [5][6][7]. This electronic tuning significantly adds complexity and power, which reduces the battery lifetime. Non-electronic tuning techniques have been studied but they require high temperature, specific gas environments, and are not reversible [8][9]. In this work, we present an *in-situ* non-electronic mechanical tuning technique involving nano-electrodeposits, which operates at room temperature, consumes very little power, and is reversible. This technique can be used to adjust microphone sensitivity to attain directionality and may be used to achieve a customized fit to a hearing aid user's needs, even after the unit leaves the manufacturing facility.

2 DEVICE DESIGN AND OPERATING PRINCIPLE

2.1 Device Design

Figure 1(a) shows a dual MEMS microphone with integrated Ag-Ge-Se solid electrolyte. The microphone has three major parts: a suspended multiple-layer diaphragm, including 3000 Å parylene, 3000 Å Au, 3 µm parylene, 3000 Å SiO_2, and 3200 Å Ag-Ge-Se layers from bottom to top, top/bottom electrodes to detect capacitance change, and cathode/anode electrodes to grow nano-electrodeposits [10]. The morphology of the Ag nano-electrodeposits (height~ 90 nm) from an electrochemically-inert cathode toward an oxidizable anode is shown in Figure 1(b). The growth rate is approximately 70 ~ 100 µm/sec at 3 V.

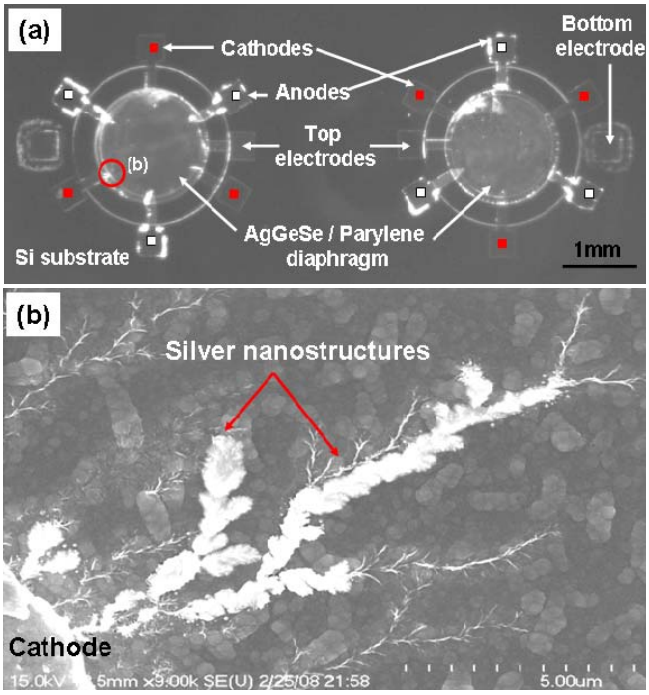

Figure 1: (a) A top view of a fabricated dual capacitive omnidirectional microphone covered by Ag-Ge-Se solid electrolyte on a suspended parylene diaphragm. (b) Grown nano-electrodeposits from a cathode on a parylene diaphragm.

2.2 Operating Principle

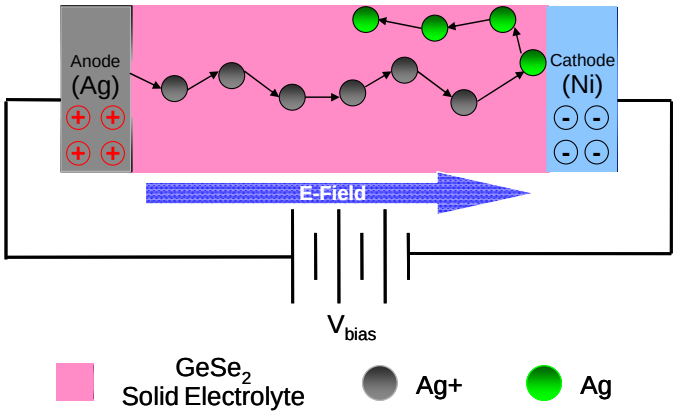

Figure 2: Schematic of an electrodeposition mechanism in Ag-Ge-Se solid electrolyte.

A schematic of the nano-electrodeposit growth process on a Ag-Ge-Se solid-state electrolyte layer is illustrated in Figure 2. An oxidizable electrode (anode) and an electrochemically-inert electrode (cathode) are placed on a Ag-doped Ge-Se film. During the oxidation process, an electron is separated from an atom, creating an ion. These charged ions move in the solid electrolyte due to an electric field supplied by an external DC bias (1 ~ 6 V). Transported ions are reduced at the cathode and the resulting electrodeposit grows toward the anode. The growth is non-volatile, operates at room temperature, and is reversible. The retraction occurs upon application of a reverse bias which results in the dissolution of the electrodeposit.

3 FABRICATION AND EXPERIMENTAL SETUP

3.1 FABRICATION

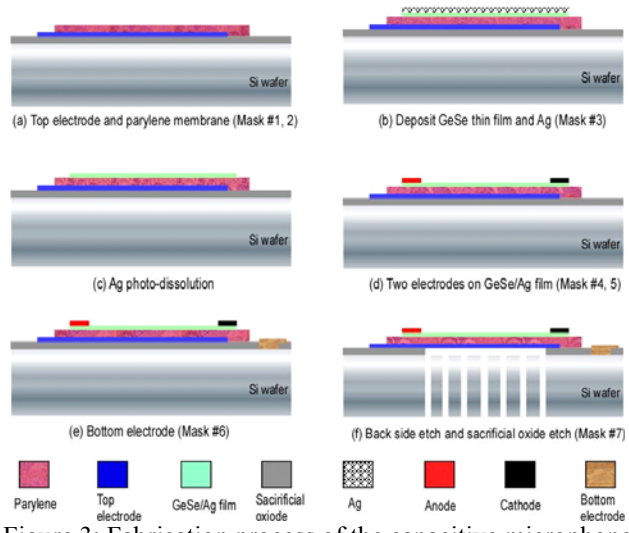

Figure 3: Fabrication process of the capacitive microphone covered by Ag-Ge-Se solid electrolyte on a suspended parylene diaphragm.

The fabrication process for integrating the capacitive microphone with the nano-electrodeposit is illustrated in Figure 3. The seven-mask process includes evaporation of the Ag-doped Ge-Se solid electrolyte on the parylene diaphragm suspended over a silicon substrate. C-type parylene is used for the diaphragm because of its excellent electrical and mechanical properties. All metal patterning is performed by a lift-off processes. (a) The suspended diaphragm has two layers of parylene. The first parylene layer (3000-Å thick) is coated on a 1-µm thick sacrificial oxide layer on the silicon wafer to provide electrical isolation between the top and bottom electrodes. The parylene layer is etched in an oxygen plasma for 1.5 min at an etch rate of 2000 Å/min under 15-sccm oxygen, 100-W RF power, and 500-V bias. A 3000-Å thick top electrode (Cr/Au) is then deposited and patterned on this first parylene layer. The second parylene layer (3-µm thick) is coated on the top electrode and patterned in an oxygen plasma for 15 min. This second parylene layer is the main structural layer of the diaphragm. (b) $Ge_{30}Se_{70}$ base glass (2400-Å thick) and silver layers (800-Å thick) are thermally evaporated sequentially without breaking vacuum inside the evaporator and patterned on the diaphragm. The optimized thickness ratio of Ge-Se to Ag to ensure the highest Ag^+ ion concentration in the electrolyte is approximately 3:1 according to previous work [11]. (c) Immediately after the deposition of the bilayer, photo-dissolution using UV exposure for 15 min diffuses silver into the Ge-Se layer to form the solid electrolyte [12]. The UV light triggers formation of charged defects that react with silver; this results in a superionic Ag-Se phase formation within the film [13]. (d) The anode (silver) and cathode (nickel) are separately evaporated and patterned on the diaphragm. (e) The bottom electrode is formed by removing the 1-µm thick oxide by buffered oxide etchant for 50 min, and Cr/Au metal films are evaporated and patterned to access the silicon substrate. (f) Finally, the diaphragm is defined by Deep Reactive Ion Etch (DRIE, STS Inc.) from the back side of the silicon wafer at an etch rate of 3 µm/min. We used a standard SF_6/C_4F_8 alternating etch process (12 sec/8 sec, 130 sccm/85 sccm) and 800 W/10 W coil/platen powers, respectively. The diaphragm is then released by using concentrated hydrofluoric acid for 15 min to remove the 1-µm sacrificial oxide layer.

3.2 EXPERIMENTAL SETUP

Experimental setup and acoustic calibration are shown in Figure 4. All of experiments have been performed in an anechoic chamber to minimize electromagnetic noise. The microphone and readout circuit are mounted on a PCB and placed inside a Faraday cage to minimize unwanted noise as shown in Figure 4(a). Two variable capacitors model the MEMS microphones. The amplified outputs of the variable capacitors are fed to a differential amplifier to read the mismatch. The readout circuit has a passband of 0.1 ~ 100 kHz and a sensitivity of 300 mV/pF. The operating

NSTI-Nanotech 2009, www.nsti.org, ISBN 978-1-4398-1782-7 Vol. 1, 2009

principle of the readout is as follows: the microphones are biased by high-impedance resistors (*R1* and *R2*, 10 MΩ) to 250 mV (*Mic_pwr by a voltage divider of R7/R8*). External acoustic excitation actuates the charged microphones diaphragms to produce voltage changes, which is modeled as a change in the variable capacitors by voltage sources (*V1* & *V5*). The voltage sources mimic acoustic excitations which have 20 pV offset voltage and 0.1 pV amplitude in a frequency band of 0.5 ~ 7 kHz. The offset voltages model the mismatch of the microphones. The induced voltage change on the microphone passes through an isolation capacitor (*C1*) as a displacement current, and is amplified by an AD8607 amplifier with 100x closed-loop gain set by *R3* and *R6*. The response of the circuit shows both high and low frequency loss. The low frequency response of the circuit is limited by charge-retention in the bias resistor. When the RC time constant is the same order of magnitude as the signal period, voltage discharge across the bias resistor dominates the circuit loss. The low frequency cutoff can be improved by using a larger resistor; however, doing so reduces the gain of the circuit. The 100 MΩ bias resistor balances the circuit bandwidth and peak output. At very high frequencies, the loss results from signal leakage as displacement current through the microphone.

Figure 4(b) shows acoustic calibration result over the wide range of incident SPL from 20 to 90 dB SPL, performed in an acoustic chamber. The readout circuit is powered by DC power supplies (to remove the periodic 60-Hz noise) with 87-dB input Sound Pressure Level (SPL) at 3 kHz. The response is very linear as a function of incident SPL (a regression (R^2) of 0.9999).

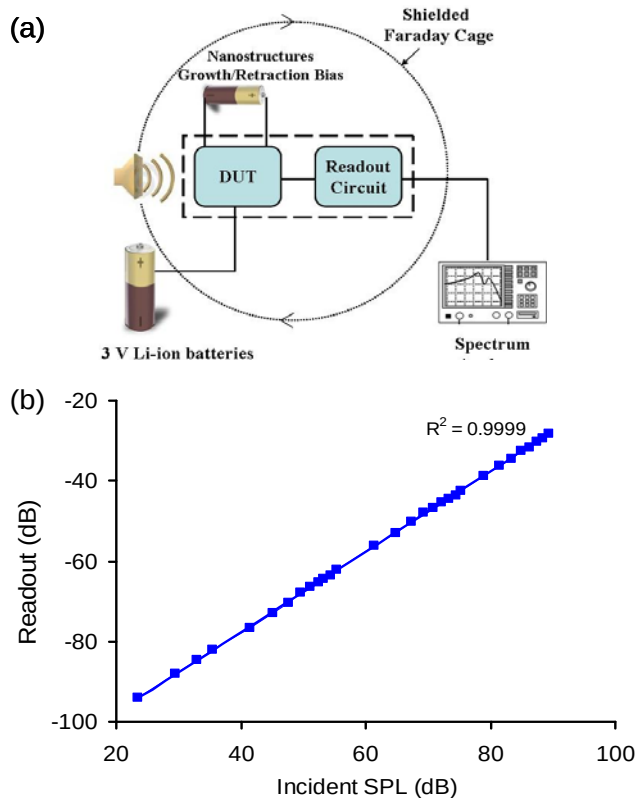

Figure 4: (a) Experimental setup to test microphone directionality: 1.5-V Li-ion batteries have been used to grow nano-electrodeposits and remove the periodic 60-Hz noise. (b) Wide range of Sound Pressure Level (SPL) versus the output of the readout circuit.

4 DEVICE CHARACTERIZATIONS

Figure 5 shows frequency responses of microphone sensitivity upon the nano-electrodeposit growth and retraction. The initial sensitivity is 34 dB after 100x amplification. The sensitivity is tuned by 2 dB and 1 dB upon the growth and retraction, respectively. Generally, in order to avoid hysteresis, the retraction bias voltage is two times higher than growth bias voltage and shorter growth time (less than 10 sec) is required. However, due to the hysteresis, frequency response after retraction doesn't return to the initial response.

Figure 6 shows acoustic polar plots, demonstrating directionality tuning of the microphone from 500 Hz to 3 kHz upon the nano-electrodeposit growth and retraction. The initial mismatch between two omni-directional MEMS microphones is 2 dB and shows 2.0 dB DI at 1 kHz. As the growth continues, the polar plot patterns become closer to "Figure 8" patterns in every frequency range, indicating high directionality. Consequently, DI is enhanced by 1.3 dB with nano-electrodeposit growth and reversed to an initial stage by retraction. This technique could be useful for self calibration and post-packaging tuning of a variety of microdevices.

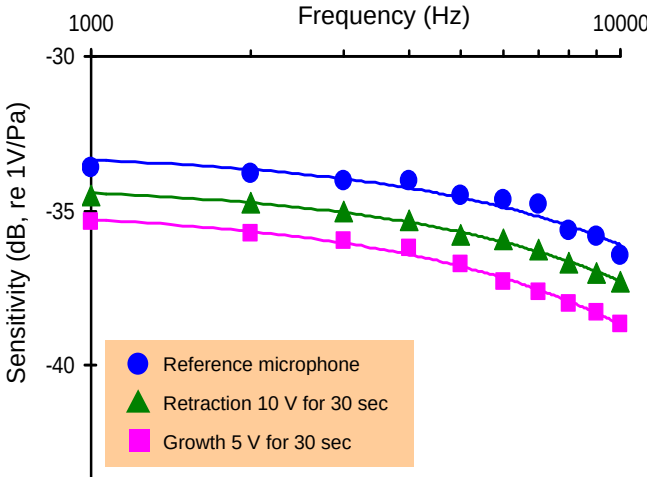

Figure 5: Frequency response over sensitivity upon nano-electrodeposit growth (5 V for 30 sec) and retraction (10 V for 30 sec).

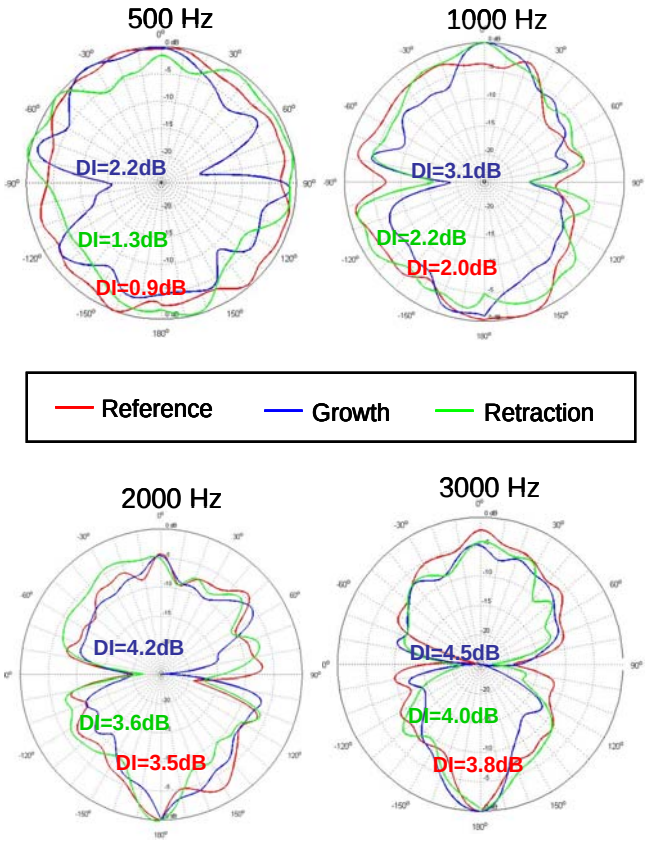

Figure 6: Directionality tuning of the dual microphone on a polar plot from 500 Hz to 3 kHz as rotation of in-plane. DI is enhanced with grown Ag nano-electrodeposits and reversed to initial stage with retracted Ag nano-electrodeposits.

5 CONCLUSION

In order to overcome existing cost-ineffective mechanical tuning techniques for MEMS devices, we demonstrate *in-situ* tuning performed by growing and retracting nano-electrodeposits on a solid electrolyte layer integrated with the suspended parylene diaphragm of a MEMS microphone for hearing aid applications. The sensitivity tuning result shows of 1.3 dB DI improvement on growth and 0.9 dB DI reversal on retraction. By manipulating the sensitivity, this technique is suitable for a hearing aid user's customized fit, removing drift and mismatch caused by the the environment in the ear canal. Also, the technique has potential in other microdevice applications, such as resonant frequency alteration, sensitivity matching, and post-packaging trimming. The *in-situ* tuning technique using integrated nano-electrodeposits offers a step toward reducing those post-production costs and minimizing existing limitations.

ACKNOWLEDGMENT

The authors would like to acknowledge Mr. Yongmo Yang, the Center for Solid State Electronics Research (CSSER) staff at Arizona State University, Prof. Tom Milster's group at University of Arizona, and Knowles electronics for their continuing support. We also appreciate the US National Science Foundation (US NSF) supporting this work under Grant #0627777 and #0652136.

REFERENCES

[1] M. C. Killon, "Myths About Hearing in Noise and Directional Microphones," *Hearing Review*, 2004.

[2] D. A. Fabry, "Adaptive Directional Microphone Technology and Hearing Aids: Theoretical and Clinical Implications," *Hearing Review*, 2005.

[3] J. Tchorz, "Effects of Microphone Mismatch in Directional Hearing Instruments**,"** *Hearing Review*, 2001.

[4] S. C. Thompson, "Dual microphones or directional-plus-omni: Which is best? In S Kochkin & KE Strom's High Performance Hearing Solutions," *Hearing Review*, vol 3, pp. 31-35, 1999.

[5] B. Widrow and F. Luo, "Microphone arrays for hearing aids: An overview," *Speech Communication*, vol. 39, pp. 139-146, 2003.

[6] J. L. Alcantara, B. C. Moore, V. Kuhnel, and S. Launer, "Evaluation of the noise reduction system in a commercial digital hearing aid," *Int. J. Audiol.*, vol. 42, pp. 34–42, 2003.

[7] T. A. Powers and V. Hamacher, "Three-microphone instrument is designed to extend benefits of directionality," *Hearing Journal*, vol. 55, pp.38–45, 2002.

[8] S. C. Jun, X. M. H. Huang, and J. Hone, "Electrothermal frequency tuning of a nano-resonator," *Electronics Letters*, vol. 45, pp. 1484-1485, 2006.

[9] D. Joachim and L. Lin, "Characterization of selective polysilicon deposition for MEMS resonator tuning," *Journal of MEMS*, vol. 12, no. 2, pp. 193-200, 2003.

[10] S. -S. Je, J. Kim, M. N. Kozicki, and J. Chae, "In-Situ Tuning of Omni-Directional Micro-Electro-Mechanical-Systems Microphones to Improve Performance Fit in Hearing Aids," *Applied Physics Letters*, 93, 123501, 2008.